NUCL SCI TECH (2021) 32:83
https://doi.org/10.1007/s41365-021-00913-y

Intra-beam scattering and beam lifetime in a candidate lattice of the soft X-ray diffraction-limited storage ring for the upgraded SSRF

Xin-Zhong Liu[1,2] · Shun-Qiang Tian[3] · Xu Wu[1,2,3] · Meng Wang[1,4] · Zhen-Tang Zhao[1,3]

Received: 2 March 2021 / Revised: 12 June 2021 / Accepted: 17 June 2021 / Published online: 6 August 2021

Abstract New-generation synchrotron light sources are being designed and operated worldwide to provide brighter radiation by reducing the beam emittance to X-ray diffraction limits. Intra-beam scattering (IBS) and Touschek scattering in such facilities are significant and require attention because of their ultra-low emittance. Therefore, cure strategies need to be carefully studied to obtain high-quality photon beams. For the Shanghai Synchrotron Radiation Facility Upgrade (SSRF-U), a candidate lattice of the storage ring, reaching the soft X-ray diffraction limit, was designed and presented for the first time in this study. The emittance growth and beam lifetime in the SSRF-U storage ring were studied using particle simulations for a series of different machine configurations. The gains with RF frequencies of 100 MHz and 500 MHz were compared. Along with a better filling pattern, a more suitable RF frequency was adopted in the SSRF-U. The variations in the equilibrium beam emittance with beam coupling and bunch-lengthening were identified using simulations. Optimal beam coupling and required bunch-lengthening for the SSRF-U storage ring were thus determined. The fitness of the beam energy in the SSRF-U was subsequently assessed using the obtained parameters. Additionally, the Touschek scattering and beam lifetime were calculated, and an acceptable total beam lifetime was obtained.

Keywords Diffraction-Limited Storage Ring (DLSR) · Shanghai Synchrotron Radiation Facility Upgrade (SSRF-U) · Intra-Beam Scattering (IBS) · Touschek scattering; Beam lifetime

✉ Shun-Qiang Tian
tiansq@sari.ac.cn

✉ Zhen-Tang Zhao
zhaozhentang@sinap.ac.cn

1 Shanghai Institute of Applied Physics, Chinese Academy of Sciences, Shanghai 201800, China

2 University of Chinese Academy of Sciences, Beijing 100049, China

3 Shanghai Advanced Research Institute, Chinese Academy of Sciences, Shanghai 201204, China

4 Shanghai University, Shanghai 200444, China

1 Introduction

Third-generation synchrotron radiation light sources have enabled great advances in the area of atomic and molecular material structures, chemistry, materials science, biology, and environmental sciences since the early 1990 s. The Shanghai Synchrotron Radiation Facility (SSRF) [1, 2], a third-generation light source located in China, has been a good experimental platform for many users in their scientific experiments for more than 10 years. In its present condition, the SSRF delivers stable and efficient operations, and its users regularly make high-impact scientific contributions. However, new-generation synchrotron light sources [3, 4], with reduced beam emittance approaching or reaching X-ray diffraction limits, have attracted the interest of many laboratories and are being actively considered in the upgrade plans of the existing facilities. When the electron beam dimensions in the phase space are smaller than the photon diffraction limit, the photon diffraction limit dominates the total source emittance observed from the user's sample and cannot be significantly reduced by electron beam emittance reduction. The synchrotron light source with these smaller electron beam dimensions then provides ultra-high-brightness and high spatial coherence of the photon with a given wavelength. This type of light source is called a diffraction-limited storage ring (DLSR). MAX-IV [5], with a source emittance of 330 pm·rad, and ESRF-EBS [6], with a source emittance of 135 pm·rad, are pioneers in the development of X-ray DLSRs and are currently in operation. The extremely high-average brightness and high spatial coherence of X-rays provided by the two facilities inspired physicists, engineers, and the user community of synchrotron light sources. Currently, many new or upgraded facilities of synchrotron light sources of this type are being constructed worldwide. For example, HEPS [7] with a beam emittance of 34 pm·rad and ALS-U [8] with 140 pm·rad are the new DLSRs, and APS-U [9] with 42 pm·rad and Sirius [10] with 250 pm·rad are the upgraded DLSRs.

Compared to third-generation light sources, the beam emittance in new-generation light sources is reduced by one or two orders of magnitude. Because of high electron density in bunches, intra-beam scattering (IBS) and Touschek scattering occurs. As a result, the light source properties deteriorate. IBS, which refers to multiple small-angle Coulomb scattering inside a bunch, increases the beam emittance and energy spread following the equilibrium mechanism between radiation damping and intra-beam scattering [11]. The increased beam emittance severely limits the photon brightness and spatial coherence that a DLSR can achieve. Touschek scattering, a large-angle Coulomb scattering between electrons, changes the direction of energy transfer from the transverse motion to the longitudinal direction and leads to electron loss [12], unlike IBS. Strong Touschek scattering results in a short beam lifetime. Thus, approaches such as lengthening the bunches by third-harmonic cavities, increasing beam coupling, and maximizing the occupation of radio frequency (RF) buckets have been adopted to resolve the problems in ALS-U [13], HEPS [14], and MAX-IV [15].

To increase the brightness and improve the light source quality for scientific experiments, the SSRF has an upgrade plan (hereafter denoted as SSRF-U). The SSRF-U aims to reach the soft X-ray diffraction limit, which requires the emittance to be lower than 80 pm·rad. To release the effects of IBS and Touschek scattering of the SSRF-U storage ring, a series of simulations through particle tracking were performed within the accelerator toolbox (AT) [16]. First, the IBS-affected emittance, bunch length, and energy spread were studied as functions of the beam coupling (defined by $\kappa = \varepsilon_y/\varepsilon_x$) at different RF frequencies. This inspection was repeated for various bunch-lengthening factors. Next, the IBS-affected emittance was studied as a function of energy for different current values. The Touschek scattering and beam lifetimes were investigated as functions of the beam coupling in the fourth section. After considering all the effects, better configurations were obtained for SSRF-U.

This paper is organized into four sections. Section 1 discusses the lattice design of the SSRF-U storage ring with emittance reaching the soft X-ray diffraction limit. Section 2 describes the effects of IBS on emittance, bunch length, and energy spread. Section 3 presents the results of the Touschek scattering and beam lifetime calculations for the SSRF-U storage ring. The conclusions are given in Sect. 4.

2 Lattice design of the SSRF-U storage ring

With advances in high-gradient magnets and high-precision alignment, light sources employing a multi-bend achromatic (MBA) lattice can now achieve ultra-low beam emittance. The hybrid MBA structure was first proposed and implemented for the ESRF-EBS project [17]. This structure has two dispersion bumps generated by the lengthening of the path between the first and second, the sixth and seventh dipoles in each cell. Using this structure, the problem of sextupole strength increasing significantly as beam emittance decreases in the standard MBA lattice can be solved. Longitudinal gradient bend (LGB) [18], combined with anti-bend [19], enables dispersion disentangling and focusing matching, which further reduces the beam emittance to the X-ray diffraction limit. The hybrid seven-bend achromatic (7BA) lattice modified with the two techniques was adopted in HEPS and APS-U and is a good choice for SSRF-U.

The lattice of the SSRF-U storage ring, designed on the beam energy of 3.0 GeV, results in a natural emittance of 53.2 pm·rad, reaching the soft X-ray diffraction limit. Because the existing tunnel will be used by the SSRF-U, the lattice has 20 $\times$ 7BA cells forming four super-periods, with a circumference of 432 m. The main parameters of SSRF-U are listed in Table 1. The beam optics and lattice layout for one super-period are shown in Fig. 1.

Each 7BA cell has seven dipoles, ten quadrupoles, and six sextupoles. The maximum gradients of the quadrupole and sextupole were 85 T/m and 5100 T/m^2, respectively. The lattice provides four long straight sections with lengths of 10.1 m, and 16 standard straight sections with lengths of 5.1 m. The horizontal and vertical tunes were optimized to be 51.17 and 16.22, respectively, away from the harmful nonlinear resonances. The horizontal and vertical β functions at the centers of long straight sections are 15.29 m and 5.67 m, while 5 m and 3 m at the centers of standard straight sections.

The momentum acceptance (MA) and dynamic aperture (DA) were obtained by particle tracking and are shown in Fig. 2(a) and (b), respectively. MA along the SSRF-U

Table 1 Main parameters of the SSRF-U storage ring (bare lattice)

Parameter	Value
Lattice	20 × 7BA
Beam energy (GeV)	3.0
Circumference (m)	432
Current (mA)	500
Tune (*H*, *V*)	51.17, 16.22
Bunch number	360
Number of particles per bunch	1.25e9
Bunch charge (nC)	2.0
Natural bunch length (mm)	2.60
RF frequency (MHz)	499.654
RF voltage (kV)	2000
Harmonic number	720
Momentum compaction factor	6×10^{-5}
Natural chromaticity (*H*, *V*)	− 98.63, − 68.11
Damping partition number (J_x, J_y, J_z)	2.27, 1.00, 0.73
Damping time (*H*, *V*, *E*) (ms)	5.98, 13.57, 18.53
Corrected chromaticity (*H*, *V*)	2.0, 1.0
Energy loss per turn (keV)	637.128
Natural energy spread	1.351×10^{-3}
Natural emittance (pm·rad)	53.22

storage ring was greater than ± 1.5%. The Touschek lifetime dominated by this momentum acceptance is given in Sect. 4. The injection point has a momentum acceptance higher than ± 2%, which is sufficient to capture all the injected electrons with energy spread. For the SSRF, the energy spread of the booster was 7.799×10^{-4}. In the simulation, the energy spread of the booster in the SSRF-U was 0.1%. The DA is approximately 2.5 mm in the horizontal plane and 2 mm in the vertical plane. Swap-out injection is applied in the SSRF-U to achieve efficient injection under this limitation (DA).

3 Intra-beam scattering (IBS)

3.1 Theory of intra-beam scattering (IBS)

IBS and multiple small-angle Coulomb scattering events among the electrons in a bunch lead to electron diffusion in the six-dimensional phase spaces. Based on the Bjorken–Mtingwa model, the IBS rate can be accurately expressed as follows [11]:

$$\frac{1}{T_i} = 4\pi A(\log)\left\langle \int_0^\infty \mathrm{d}\lambda \frac{\lambda^{1/2}}{[\det(L+\lambda I)]^{1/2}} \times \left\{ TrL^i Tr\left(\frac{1}{L+\lambda I}\right) - 3Tr\left[L^i\left(\frac{1}{L+\lambda I}\right)\right]\right\}\right\rangle, \tag{1}$$

where i represents p, h, v; T_p is the growth time of the relative energy spread, T_h is the growth time of the horizontal emittance, T_v is the growth time of the vertical emittance, (log) is the Coulomb logarithm, and I is the unit matrix. A is calculated as follows:

$$A = \frac{r_0^2 cN}{64\pi^2\beta^3\gamma^4\varepsilon_\mathrm{h}\varepsilon_\mathrm{v}\sigma_\mathrm{s}\sigma_\mathrm{p}}, \tag{2}$$

where r_0 is the classical electron radius, c is the speed of light, N is the number of particles in each bunch, β is the particle velocity divided by c, ε_h and ε_v are the transverse emittances, γ is the particle energy divided by the rest mass, σ_s is the bunch length, and σ_p is the relative energy spread.

Based on the analysis of Eqs. (1) and (2), we can conclude that reducing the density of electrons is an

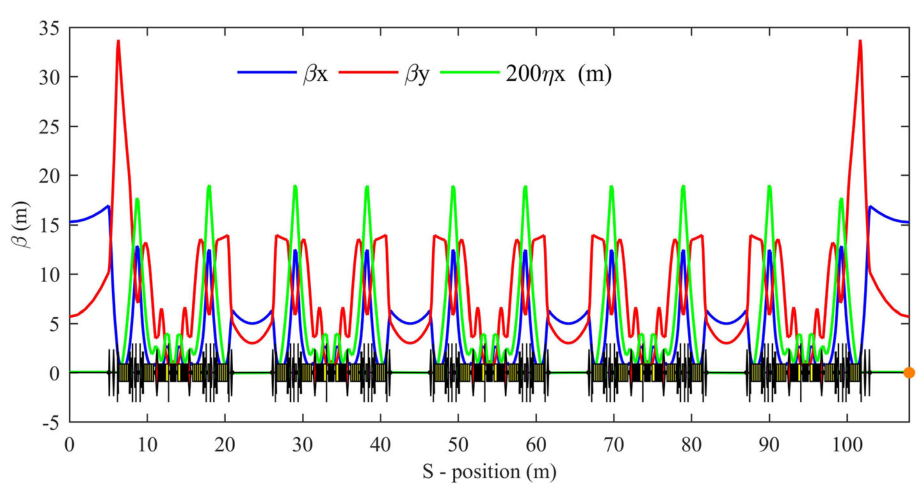

Fig. 1 (Color online) Linear optical functions of the designed SSRF-U storage ring @ standard super-cell

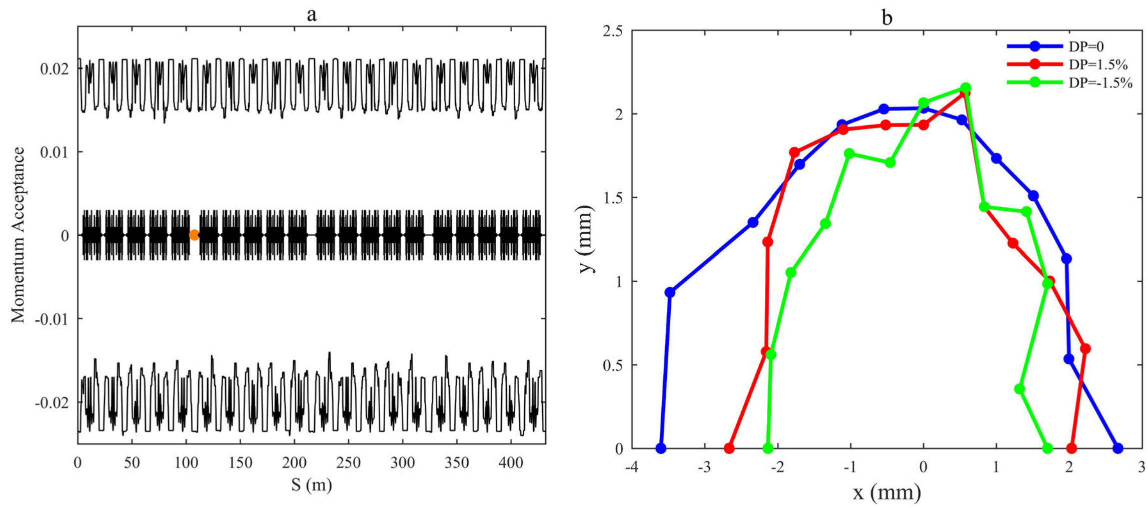

Fig. 2 (Color online) Momentum acceptance (left) and dynamic aperture (right) of the SSRF-U

appropriate way to weaken the IBS effects. The following subsections describe our strategies for determining an optimal setting for the SSRF-U.

3.2 Equilibrium beam parameters with IBS effect

The code IbsEmittance developed by implementing the Bjorken–Mtingwa model [14] was applied to evaluate the influence of IBS. The equilibrium beam parameters influenced by IBS were calculated, and the values are summarized in Table 2. For further investigation, the equilibrium transverse emittances as functions of coupling, the beam current, coupling under a fixed current $I = 500$ mA, and beam current for different couplings of the SSRF-U were calculated, as shown in Fig. 3(a)–(d), respectively.

Considering the third-generation light source, beam coupling is generally set to 1% or < 1%. However, the simulation results in Table 2 indicate that the horizontal and vertical emittance at 500 mA are approximately three times higher than those at zero current with coupling = 1%. The emittance growth resulting from IBS becomes too large to be acceptable for the SSRF-U storage ring when the coupling is set to 1%. As shown in Fig. 3(a) and (b), upon increasing the coupling to 10% or higher, the effect of IBS will be weakened to an acceptable level. Therefore, increasing the coupling to 10% or higher is considered to weaken the IBS and influence of prioritization schemes. When the coupling is set to 10%, the equilibrium horizontal emittance can be reduced to 95.54 pm·rad and the energy spread to 0.165%. Therefore, increasing the coupling to weaken the effect of IBS is a good choice, and it may be interesting to investigate the full coupling in future studies.

Table 2 Equilibrium beam parameters for the SSRF-U with IBS effect

Parameter	$\kappa = 1\%$	$\kappa = 1\%$	$\kappa = 10\%$	$\kappa = 10\%$
Beam current (mA)	0	500	0	500
Emit_x (pm·rad)	52.81	149.48	48.46	95.54
Emit_y (pm·rad)	0.5281	1.489	4.846	9.554
Energy spread ($\times 10^{-3}$)	1.35	1.86	1.35	1.65
Bunch length (mm)	2.60	3.57	2.60	3.18

3.3 IBS effects with different RF frequencies

Because of the limited DA, beam injection in the SSRF-U storage ring is planned to be realized by the swap-out injection method without using an accumulation ring, as in APS-U [20]. A lower RF frequency can reduce the difficulty of manufacturing a fast-pulsed kicker, such as a required pulse width of 10 ns for an RF frequency of 100 MHz. However, this can lead to a filled-bunch reduction, which may significantly increase the electron density in a bunch and aggravate the IBS effect in the filling mode with high-average brightness. To overcome this difficulty in the SSRF-U storage ring, a novel pattern in which three bunches are filled in every five buckets at an RF of 500 MHz was proposed. This type of filling pattern improves the operation of the injection system with a long pulse and allows more electron bunches to rotate around the ring. The booster of the SSRF can continuously supply three bunches of the same energy. Therefore, in the future, the booster of the SSRF-U could supply three bunches of the same energy. Considering the current fast pulse technology of the injection system, the rise and fall times and flat time of the buckets for RF frequencies of 100 MHz and

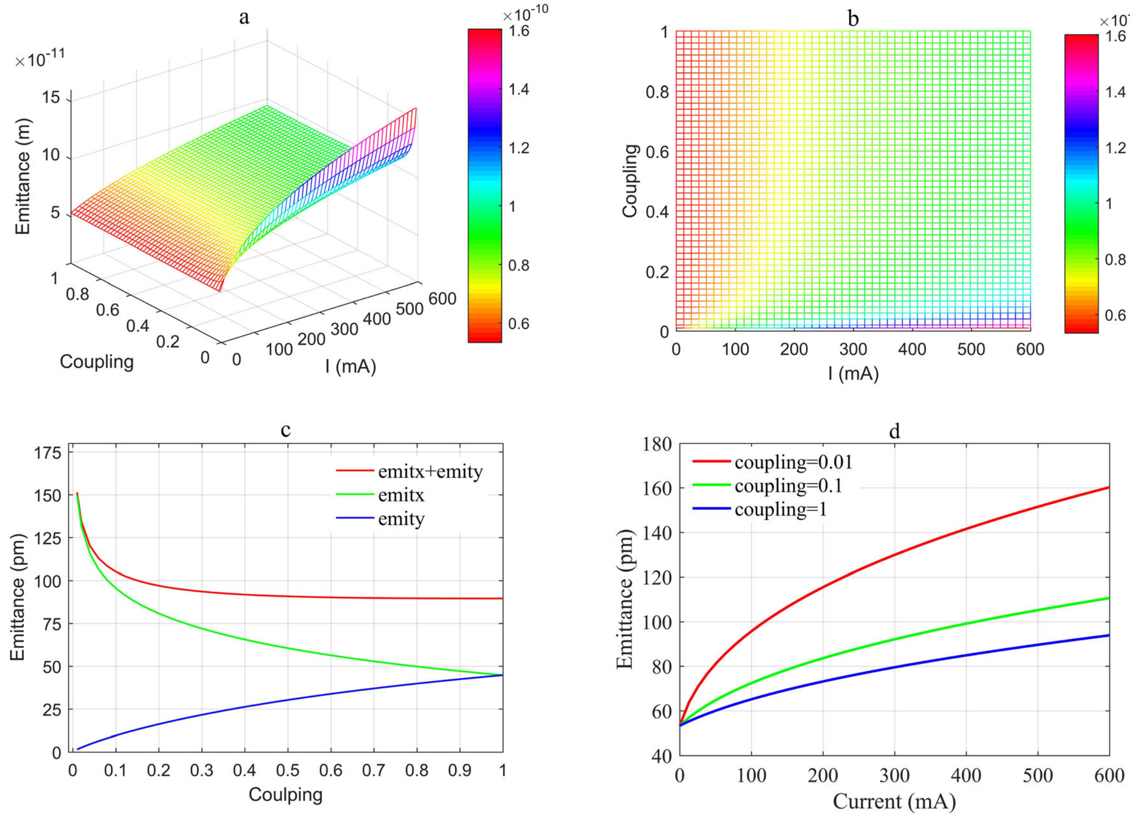

Fig. 3 (Color online) Illustration of estimated equilibrium transverse emittances vs. coupling and beam current (a, b). Equilibrium transverse emittances as a function of the coupling of the SSRF-U for I = 500 mA (c). Equilibrium transverse emittances vs. the beam current for different couplings of the SSRF-U (d)

500 MHz are given in Table 3 [21]. In the beam-filled mode, three of the five buckets were filled with an RF frequency of 500 MHz, as shown in Fig. 4(a).

To meet different requirements of the users and achieve a stable operation of the beam, two types of filling patterns are planned in the SSRF-U, which includes the high-average brightness mode and the mode of high charge in a single bunch. The IBS effect was investigated in four cases: (1) high-brightness mode, 500 mA, 360 bunches, 2 nc/bunch, an RF frequency of 500 MHz; (2) high-brightness mode, 500 mA, 100 bunches, 7.2 nc/bunch, and an RF frequency of 100 MHz; (3) high-bunch charge mode, 20 mA, 25 bunches, 28.8 nc/bunch, and an RF frequency of 500 MHz; (4) high-bunch charge mode, 20 mA, 25 bunches, 28.8 nc/bunch, and an RF frequency of 100 MHz. The results were compared, and the choices of RF frequency and filling pattern were evaluated. The bunch lengths for the zero beam at 500 MHz and 100 MHz are 2.6 mm and 5.88 mm, respectively. The beam emittance, energy spread, and bunch length as functions of the beam coupling in the SSRF-U storage ring for the abovementioned four cases are shown in Fig. 4(b)–(d), respectively.

Table 3 Pulser parameters with RF frequencies of 100 MHz and 500 MHz

Parameters	100 MHz	500 MHz
Pulse total width (ns)	14	14
Rise and fall time (ns) (10–90%)	6	4
Flat top (ns) (> 90%)	2	6

The simulation results show that operating at frequencies of 500 MHz and 100 MHz is favorable for the high-brightness and high-bunch charge modes, respectively. Additionally, the number of users in the high-brightness mode is much greater than that of the others, and the high-brightness beam-filling pattern at 500 MHz is better than that at 100 MHz for the SSRF-U storage ring. Therefore, the use of an RF frequency of 500 MHz is preferable for SSRF-U. Maximizing the occupation of the RF buckets is useful for decreasing the influence of IBS. If the rise and fall times can be further reduced, we consider that four of the five buckets can be filled in the high-brightness beam-filling pattern with a frequency of 500 MHz. The SSRF-U can be operated with 480 bunches, and the IBS effect can be further weakened.

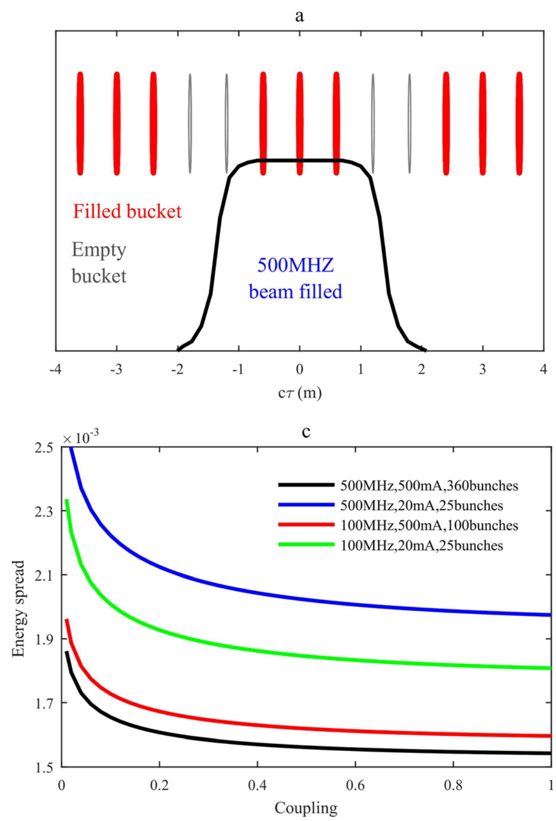

Fig. 4 (Color online) Beam-filling pattern with an RF frequency of 500 MHz (a); The beam emittance, energy spread and bunch length as functions of the beam coupling in the SSRF-U storage ring with the four cases are shown in (b), (c), and (d) respectively; The solid line represents emit$_x$ and the dotted line represents emit$_y$ (b)

3.4 IBS effects with bunch-lengthening

Bunch-lengthening is also a reasonable method to weaken the effects of IBS. Third-harmonic cavities have been used in many synchrotron radiation light sources to lengthen the electron bunch [22–24]. Theoretically, the maximum-lengthening factor in the SSRF-U storage ring with a single third-harmonic cavity is nine. However, this value is difficult to achieve using a real machine. Therefore, the bunch-lengthening factor was chosen as five or smaller for the SSRF-U storage ring. The bunch length of the SSRF-U can be extended to 13.0 mm.

The emittance and energy spread variations with beam coupling were calculated for the high-average-brightness operation mode in the SSRF-U. The results are plotted in Fig. 5, in which the three-factor and five-factor bunch-lengthening cases are compared with the case of no bunch-lengthening. When the electron bunch is lengthened by a factor of five with a coupling of 10%, the emittance growth can be decreased from 80% to approximately 20%, and the energy spread also decreased, as shown in Fig. 5(a) and (b), respectively. The figure shows that the five-factor bunch-lengthening is a good choice for the SSRF-U because of the lower emittance and energy spread growth.

3.5 Fitness of the beam energy

Based on the theory of synchrotron radiation and quantum excitation, we know that for a given lattice, if only the interaction between radiation damping and quantum excitation is considered, the equilibrium emittance can be calculated as follows [25]:

$$\varepsilon_{x_0} = C_{\mathrm{q}} \frac{\gamma^2}{J_x} \frac{I_{\mathrm{s}}}{I_2}, \tag{3}$$

$$C_{\mathrm{q}} = \frac{55}{32\sqrt{3}} \frac{\mathrm{h}}{\mathrm{mc}}, I_2 = \int \frac{\mathrm{d}s}{\rho^2}, I_5 = \int \frac{\mathrm{H}_{\xi}}{\rho^3} \mathrm{d}s, \tag{4}$$

where I_2 and I_5 are the integrals of synchrotron radiation, J_x is the horizontal damping partition number, and ρ is the radius of the bend. Equations (1) and (2) show that the IBS growth rate is approximately inversely proportional to the fourth power of the beam energy, whereas Eq. (3) shows that the natural emittance of the beam is directly proportional to the square of the beam energy. Therefore, an optimized energy value can be obtained by considering the combined effect of the IBS effect, synchrotron radiation damping, and quantum excitation effect. The equilibrium emittance of the SSRF-U was the minimum at this energy.

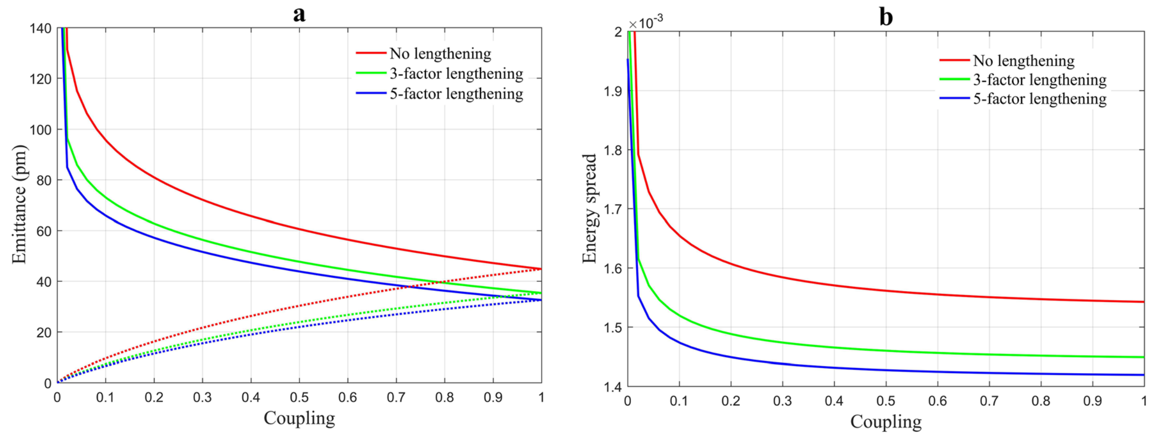

Fig. 5 (Color online) Equilibrium transverse emittances (left) and relative energy spread (right) for different bunch lengths as a function of the coupling of the SSRF-U. The solid line represents emit$_x$ and the dotted line represents emit$_y$

Based on the analysis of Eqs. (1), (2), and (3), the relationship between the equilibrium emittance and beam energy was compared for different beam currents in the SSRF-U storage ring. The value of the transverse coupling was set to 10%, and the bunch length was set to 13.0 mm in the simulation. The variation in the equilibrium emittance with the beam energy is shown in Fig. 6 for different values of current.

After conducting a similar analysis to that of Eqs. (1), (2), and (3), an optimized energy value for the equilibrium emittance can be estimated. The minimum value of the equilibrium emittance for the SSRF-U is located near 3.0 GeV in the high-brightness beam-filling pattern, as shown in Fig. 6. Additionally, it can be observed that when the energy is low, the equilibrium emittance is significantly affected by the IBS effect. The IBS effect and synchrotron radiation damping have a large influence on the equilibrium emittance. The IBS effect of SSRF-U can be neglected when operating at high energies. Therefore, the optimum energy value for the SSRF-U design should exceed 2.5 GeV. Considering the spectral coverage range of the existing beam line, the ID brightness increases with an increase in the beam energy for the same ID. Thus, it can be concluded that operation at an energy of 3.0 GeV and a beam current of 500 mA is not only better for the users but also beneficial for the beam performance in the SSRF-U.

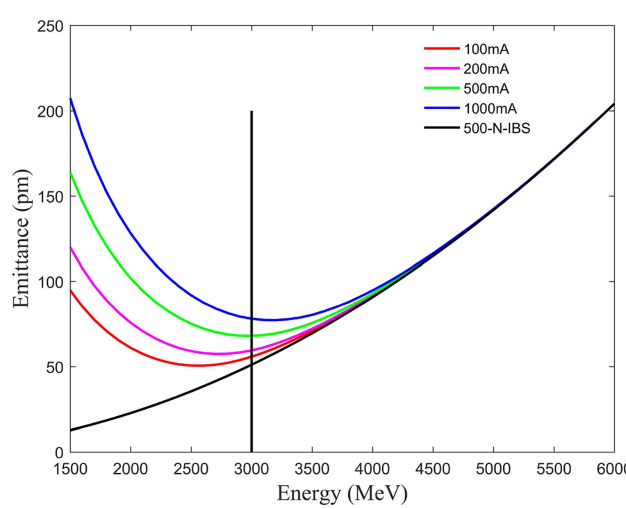

Fig. 6 (Color online) Emittance as a function of energy for the SSRF-U design. The colored curves correspond to different current values

4 Beam lifetime

The 1/e beam lifetime, defined as the duration of beam current decay to e^{-1} of the initial beam current, mainly consists of three parts with different beam loss mechanisms in the synchrotron light source, and can be calculated as follows:

$$\frac{1}{\tau_{\text{totle}}} = \frac{1}{\tau_{\text{Touschek}}} + \frac{1}{\tau_{\text{gas}}} + \frac{1}{\tau_{\text{quantum}}}, \tag{5}$$

where τ_{total} is the total lifetime, τ_{Touschek} is the Touschek lifetime, τ_{gas} is the gas-scattering lifetime, and τ_{quantum} is the quantum lifetime. The gas-scattering lifetime comprises the elastic scattering lifetime and inelastic scattering lifetime. The Touschek lifetime dominated the beam lifetime for the SSRF. Compared with the SSRF, the SSRF-U has a much smaller beam emittance and higher beam current. Thus, the Touschek scattering effect will be much stronger. DA influences the gas-scattering lifetime, which could be another factor that could reduce the beam lifetime. Because the DA in the SSRF-U is very small, particularly considering the tolerance, attention needs to be paid to the elastic scattering lifetime. The ratio of the physical aperture to the beam size primarily determines the quantum lifetime. This is too long to be considered for the SSRF-U storage ring.

In the following sections, the Touschek lifetime, elastic scattering lifetime, and inelastic scattering lifetime are calculated, and prioritization schemes for increasing the beam lifetime are designed. Subsequently, the total beam lifetime is obtained.

4.1 Touschek lifetime

Touschek scattering is a large-angle Coulomb scattering between the electrons in a beam bunch, causing momentum transport from the transverse motion to the longitudinal direction, which increases the longitudinal momentum outside the momentum aperture or the RF bucket and leads to particle loss. The calculation formula of the Touschek lifetime derived by Piwinski is shown in Eq. (6) [26].

$$1/\tau_{\mathrm{Touschek}} = \left\langle \frac{r_0^2 c N_{\mathrm{b}}}{8\pi\gamma^2\sigma_{\mathrm{s}}} F(\delta_{\mathrm{m}}, B_1, B_2) \frac{1}{\sqrt{\sigma_x^2\sigma_y^2 - \sigma_\delta^4 D_x^2 D_y^2 \beta\delta_{\mathrm{m}}}} \right\rangle, \tag{6}$$

where r_0 is the classical electron radius, c is the speed of light in vacuum, N_{b} is the number of particles in each bunch, γ is the Lorentz factor, σ_{s} is the bunch length, δ_{m} is the momentum acceptance, σ_x and σ_y are the transverse beam sizes, and F is a function of the Twiss parameter and momentum acceptance.

Equation (6) shows that the average Touschek scattering lifetime is determined by the Twiss parameter, electron density, energy acceptance, and beam size. The momentum acceptance δ_{m} along the SSRF-U storage ring was greater than $\pm$ 1.5%, as shown in Fig. 2(a). The equilibrium emittance, bunch length, and energy spread were computed using the IbsEmittance program within AT. These data and the Toucheklifetime program were used to calculate the Touschek lifetime in the high-brightness filling pattern (500 MHz, 360 buckets, and 500 mA). In the initial calculation, the coupling was 10%, and σ_{s} was 3.3 mm. However, the Touschek scattering lifetime is only 0.69 h, which is too short for the stable operation of the SSRF-U storage ring.

Increasing beam coupling and lengthening the electron bunch is necessary to increase the Touschek lifetime in the SSRF-U storage ring. Different bunch lengths versus the coupling for the Touschek lifetime and Touschek scattering rates along the ring in the SSRF-U storage ring were determined within AT. The Touschek lifetimes for different bunch lengths and different couplings in the high-brightness mode (500 MHz, 360 buckets, 500 mA) are shown in Fig. 7(a). The Touschek scattering rate distribution along the ring is shown in Fig. 7(b).

From Fig. 7(a), it can be observed that when the bunch is five times longer than the natural bunch in the high-brightness mode with a coupling of 10%, the Touschek lifetime is 2.5 h. The Touschek scattering rate of the bending section is larger than that in the other sections of the SSRF-U storage ring, as shown in Fig. 7(b). Lengthening the bunch by a factor of five can increase the Touschek lifetime and significantly reduce the Touschek scattering rate of the bending section. Moreover, if the local full coupling of the curved section can be achieved, the beam lifetime can be further improved.

4.2 Residual gas-scattering lifetime

Two dominant processes contribute to residual gas scattering, namely elastic and inelastic scattering. In the following, only elastic scattering on nuclei and inelastic scattering on nuclei (bremsstrahlung) of the residual gas-scattering lifetime component are calculated.

Elastic scattering lifetime: The elastic scattering between residual gas nuclei in the vacuum chamber and the particles of beam bunches likely increases the amplitude of the transverse oscillation. If the oscillation amplitude changes sufficiently, it causes an electron loss. The elastic scattering lifetime is the electron loss due to the elastic scattering between the residual gas nuclei and the particles of beam bunches.

The elastic scattering lifetime can be calculated as follows [27]:

$$\frac{1}{\tau_{\mathrm{elastic}}} = \frac{2\pi r_0^2 c N_{\mathrm{A}} P[\mathrm{Pa}]}{R\gamma^2 T[\mathrm{K}]} \int \frac{\beta_{x,y}}{A^{\min}[\mathrm{m}\cdot\mathrm{rad}]} \sum\nolimits_i^n Z_i(Z_i+1) N_i r_{\mathrm{p}i}, \tag{7}$$

where N_{A} is Avogadro's number, P (Pa) is the pressure, R = 8.314 J / (K$\cdot$ mol), γ is the Lorentz factor, T(K) is the temperature of the residual gas, r_{pi} is the residual gas component partial fraction, Z_i is the atomic number, N_i is the number of atoms in each molecule, and $A^{\min}$ is the transverse acceptance, which can be calculated using DA and the physical aperture. The circular dimension of the normal vacuum chamber is 10 mm $\times$ 10 mm, and the DA is about 2.5 mm in the horizontal plane and 2 mm in the vertical plane, as shown in Fig. 2(b).

Inelastic scattering lifetime: Inelastic scattering (bremsstrahlung) between the electrons in the beam bunches and the nuclei of the residual gas likely leads to electron deceleration and radiating electromagnetic waves. If the radiation energy is sufficiently large, the electrons will be beyond the range of momentum acceptance and will be subsequently lost.

The lifetime due to inelastic scattering can be calculated using the following equations [27]:

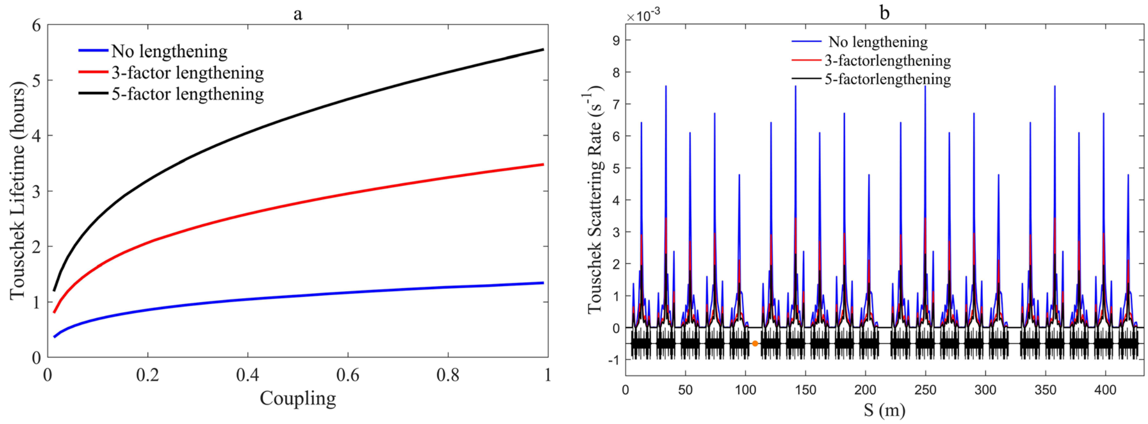

Fig. 7 (Color online) Touschek lifetimes for different bunch lengths versus coupling of the SSRF-U (a). Touschek scattering rates along the ring for different bunch lengths in the SSRF-U (b)

$$\frac{1}{\tau_{\text{inelastic}}} = \frac{4\pi r_0^2 c N_A P[\text{Pa}]}{137RT[\text{K}]} \sum_i^n \ln\frac{183}{Z_i^{1/3}} Z_i(Z_i + \xi_i) r_{\text{pi}} N_i, \tag{8}$$

with

$$\xi_i = \ln\left(1440 Z_i^{-2/3}\right) / \ln\left(183 Z_i^{-1/3}\right), \tag{9}$$

$$L(\delta_m) = 4/3 \cdot \left(\ln\left(\frac{1}{\delta_m}\right) - \frac{5}{8}\right), \tag{10}$$

where δ_m is the momentum acceptance, which is explained in Sect. 2, and the other variables are explained in the section on elastic scattering lifetime. The residual gas lifetime and the total beam lifetime with different bunch lengths are calculated using Eqs. (5), (7), (8), (9), and (10). The elastic scattering lifetime, inelastic scattering lifetime, and the total gas-scattering lifetime versus pressure are shown in Fig. 8.

It was assumed that the total pressure of the residual gas was 1 nTorr. The residual gas composition was 75% H_2, 15% CO, 7% CO_2, and 4% CH_4, which was a uniformly distributed mixture in the full ring of the SSRF-U. The temperature of the residual gas was 300 K. The elastic scattering lifetime is 131.3 h, while the inelastic scattering lifetime is 163.1 h, as shown in Fig. 8. The total beam lifetime for the SSRF-U was 2.42 h under the following conditions: operation in the high-brightness beam-filling pattern with RF of 500 MHz, beam current of 500 mA, and 360 bunches; the beam length increased by a factor of five times and the transverse coupling was 10%. A beam lifetime of 2.42 h could be sufficient for radiation safety, and the injection frequency can be achieved in the SSRF-U storage ring.

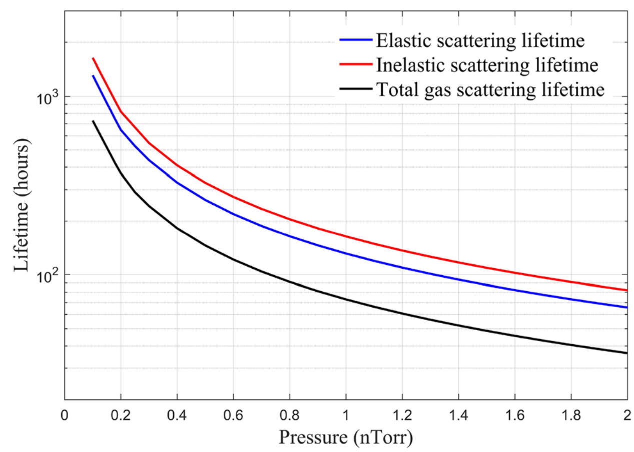

Fig. 8 (Color online) Elastic scattering lifetime, inelastic scattering lifetime and the total gas-scattering lifetime versus pressure at the SSRF-U

5 Conclusion

The lattice of the SSRF-U storage ring was designed with twenty 7BA cells forming four super-periods, resulting in a natural emittance of 53.2 pm·rad that reaches the soft X-ray diffraction limit. The DA of the SSRF-U storage ring was 2.5 mm, which was sufficient to efficiently inject the beam using the swap-out method. The results of the particle simulation studies show that operating in the high-brightness mode with an RF frequency of 500 MHz, beam current of 500 mA, and 360 bunches is suitable for the SSRF-U storage ring in terms of the beam performance and user requirements of high brightness. Additionally, the bunch length should be increased by a factor of five times using a third-harmonic cavity, and the coupling should be increased to 10% for the SSRF-U storage ring. When the SSRF-U operates in this beam-filling pattern, the energy is set to 3.0 GeV, and the total beam lifetime will be longer than 2 h. Additionally, our objective for the beam emittance to reach the soft X-ray diffraction limit can be achieved in these configurations. The new lattice of the SSRF-U can provide a lower beam emittance and higher brightness for scientific experiments than the SSRF.

Acknowledgements The authors would like to thank Dr. Na Wang and Sai-Ke Tian in IHEP for their useful discussions.

Author contributions All authors contributed to the study conception and design. Material preparation, data collection and analysis were performed by Xin-Zhong Liu, Shun-Qiang Tian, Xu Wu, Meng Wang and Zhen-Tang Zhao. The first draft of the manuscript was written by Xin-Zhong Liu, and all authors commented on previous versions of the manuscript. All authors read and approved the final manuscript.

References

1. H.J. Xu, Z.T. Zhao, Current status and progresses of SSRF project. Nucl. Sci. Tech. **19**, 1–6 (2008). https://doi.org/10.1016/S1001-8042(08)60013-5
2. L.X. Yin, R.Z. Tai, Z.T. Zhao et al., Progress and future of Shanghai synchrotron radiation facility. J. Vac. Soc. **59**, 198–204 (2016). https://doi.org/10.3131/jvsj2.59.198
3. R. Hettel, DLSR design and plans: an international overview. J. Syn. Rad. **21**, 843 (2014). https://doi.org/10.1107/S1600577514011515
4. M. Borland, G. Decker, L. Emery et al., Lattice design challenges for fourth-generation storage-ring light sources. J. Syn. Rad. **21**, 912 (2014). https://doi.org/10.1107/S1600577514015203
5. P.F. Tavares, E. Al-Dmour, Å. Andersson et al., Commissioning and first-year operational results of the MAX IV 3 GeV ring. J. Syn. Rad. **25**, 1291–1316 (2018). https://doi.org/10.1107/S1600577518008111
6. P. Raimondi, ESRF-EBS: The extremely brilliant source project. Sync. Rad. News **29**, 8–15 (2016). https://doi.org/10.1080/08940886.2016.1244462
7. Y. Jiao, G. Xu, X.H. Cui et al., The HEPS project. J. Syn. Rad. **25**, 1611 (2018). https://doi.org/10.1107/S1600577518012110
8. C. Steier, A. Allézy, A. Anders et al., Status of the Conceptual Design of ALS-U, *In Proc. 9th Int. Particle Accelerator Conf.* Vancouver, BC, Canada, April 29-May 4, (2018). https://doi.org/10.18429/JACoW-IPAC2018-THPMF036
9. Y. Sun, M. Borland, Alternate lattice design for advanced photon source multi-bend achromat upgrade, In Proceedings of IPAC2015, Richmond, VA, USA, 3–8 May (2015). https://doi.org/10.18429/JACoW-IPAC2015-TUPJE071
10. L. Liu, R.T. Neuenschwander, A.R.D. Rodrigues, Synchrotron radiation sources in Brazil. Phil. Trans. R. Soc. A **377**, 20180235 (2019). https://doi.org/10.1098/rsta.2018.0235
11. K. Kubo, K. Oide, Intrabeam scattering in electron storage rings. Phys. Rev. Spec. Top. AC **4**, 124401 (2001). https://doi.org/10.1103/PhysRevSTAB.4.124401
12. A. Xiao, M Borland, Touschek effect calculation and its application to a transport line, *In 2007 IEEE PAC*, Albuquerque, NM, USA, 25–27 June (2007). https://ieeexplore.ieee.org/document/4440456
13. C. Steier, J.M. Byrd, SD. Santis et al., Physics design progress towards a diffraction limited upgrade of the ALS, *In Proceedings of IPAC2016*, Busan, Korea, May (2016). https://www.osti.gov/biblio/1339967
14. S.K. Tian, Q.J. Wang, G. Xu et al., Intra-beam scattering studies for low emittance at BAPS. Chin. Phys. C **39**, 067001 (2015). https://doi.org/10.1088/1674-1137/39/6/067001
15. S.C. Leemann, Interplay of Touschek scattering, intrabeam scattering, and rf cavities in ultralow-emittance storage rings. Phys. Rev. Accel. Bea. **17**, 050705 (2014). https://doi.org/10.1103/PhysRevSTAB.17.050705
16. A. Terebilo, Accelerator toolbox for MATLAB. (2001). https://doi.org/10.2172/784910
17. L. Farvacque, N. Carmignani, J. Chavanne et al., A low-emittance lattice for the ESRF, *In Proceedings of IPAC2013*, Shanghai, China, 12–17 May (2013). https://accelconf.web.cern.ch/IPAC2013/papers/mopea008.pdf
18. R. Nagaoka, A.F. Wrulich, Emittance minimisation with longitudinal dipole field variation. Nucl. Instrum. Meth. A **575**, 292 (2007). https://doi.org/10.1016/j.nima.2007.02.086
19. A. Streun, The anti-bend cell for ultralow emittance storage ring lattices. Nucl. Instrum. Meth. A **737**, 148 (2014). https://doi.org/10.1016/j.nima.2013.11.064
20. A. Xiao, V. Sajaev, Simulation study of injection performance for the Advanced Photon Source upgrade, *In Proceedings of IPAC2015,* Richmond, VA, USA, 3–8 May (2015). https://accelconf.web.cern.ch/IPAC2015/papers/tupje075.pdf
21. C. Steier, A. Anders, T. Luo et al., On-axis swap-out R&D for ALS-U, *In Proceedings of IPAC2017,* Copenhagen, Denmark, 14–19 May (2017). http://accelconf.web.cern.ch/ipac2017/papers/wepab103.pdf
22. T. Phimsen, B.C. Jiang, H.T. Hou et al., Improving Touschek lifetime and synchrotron frequency spread by passive harmonic cavity in the storage ring of SSRF. Nuc. Sci. Tech. **28**, 108 (2017). https://doi.org/10.1007/s41365-017-0259-y
23. R. Nagaoka, K. Karl, F. Bane, Collective effects in a diffraction-limited storage ring. Jour. Sync. Rad. **21**, 937 (2014). https://doi.org/10.1107/S1600577514015215
24. S.K. Tian, Q.J. Wang, Y. Jiao, Bunch length manipulation in a diffraction-limited storage ring. Chin. Phys. C **39**, 127001 (2015). https://doi.org/10.1088/1674-1137/39/12/127001
25. M. Sands, Physics of Electron Storage Rings: an Introduction. Stanford Linear Accelerator Center, Calif, 1–172 (1970). https://doi.org/10.2172/4064201
26. A. Piwinski, The Touschek effect in strong focusing storage rings. Cern Library Record (1999). https://arxiv.org/pdf/physics/9903034.pdf
27. M. Zisman, ZAP user's manual, LBL-21270, Lawrence Berkeley Lab., CA, USA, (1986). https://doi.org/10.2172/6609901